

RADIAL TEMPERATURE PROFILES OF 11 CLUSTERS OF GALAXIES OBSERVED WITH *BEPPOSAX*

JIMMY A. IRWIN¹ AND JOEL N. BREGMAN

Department of Astronomy, University of Michigan,
Ann Arbor, MI 48109-1090

E-mail: jirwin@astro.lsa.umich.edu, jbregman@umich.edu

Draft version October 30, 2018

ABSTRACT

We have derived azimuthally-averaged radial temperature profiles of the X-ray gas contained within 11 clusters of galaxies with redshift $z = 0.03 - 0.2$ observed with *BeppoSAX*. Each of the 11 clusters have had their radial temperature profiles previously determined with *ASCA*. We find that the temperature profiles of these clusters are generally flat or increase slightly out to $\sim 30\%$ of the virial radius, and that a decline in temperature of 14% out to 30% of the virial radius is ruled out at the 99% confidence level. This is in accordance with a previous *ROSAT* PSPC study and an *ASCA* study by White (1999), but in disagreement with an *ASCA* study by Markevitch et al. (1998) that found on average that cluster temperature profiles decreased significantly with radius.

Subject headings: cooling flows — galaxies: clusters — intergalactic medium — X-rays: galaxies

1. INTRODUCTION

Knowledge of the radial temperature profile of the hot gas contained within galaxy clusters is a crucial element in determining the total gravitational mass of clusters. Through the equation of hydrostatic equilibrium, the total mass of the cluster can be derived if the density gradient, temperature, and temperature gradient of the gas is known. The latter quantity is the most difficult quantity to obtain, and it has generally been assumed that the gas is isothermal in most previous approaches, since collimated X-ray instruments such as *Ginga* and *EXOSAT* could not determine the temperature structure of clusters.

The assumption of isothermality of the hot gas has been called into question in recent years, mainly as a result of studies done with *ASCA*. The ability of *ASCA* to perform spatially-resolved spectroscopy over the 1–10 keV energy range made it the first X-ray instrument capable of addressing the issue of temperature structure in hot clusters. Many *ASCA* studies have found that the gas within clusters is not isothermal, but decreases with increasing radius, in some cases up to a factor of two (e.g., Markevitch 1996; Markevitch et al. 1998; Markevitch et al. 1999). However, other studies of clusters using *ASCA* data have come to the conclusion that the gas is largely isothermal (e.g., White 1999; Fujita et al. 1996; Ohashi et al. 1997; Kikuchi et al. 1999), at least outside of the cooling radius of cooling flow clusters. A likely cause of this discrepancy is the handling of the large, energy-dependent point spread function (PSF) of *ASCA* that preferentially scatters hard X-rays. This creates an artificial increase in the temperature profile with radius if not dealt with properly. The PSF-correction method applied by Markevitch et al. consistently leads to significantly decreasing temperature profiles, while other methods (most notably the method of White 1999) lead to isothermal profiles.

The discrepancy among the different PSF-correction methods prompted an analysis of *ROSAT* PSPC data by Irwin, Bregman, & Evrard (1999). Although *ROSAT* was

only sensitive to photon energies up to 2.4 keV and was therefore not the most ideal instrument with which to study hot clusters, large (factor of two) differences in temperature should have been detected, but were not. The composite X-ray “color” profiles for 26 clusters in the Irwin et al. (1999) survey indicated isothermality outside of the cooling radius. In fact, a 20% temperature drop within 35% of the virial radius was ruled out at the 99% confidence level.

In this paper, we attempt to resolve the temperature profile discrepancy using *BeppoSAX* data. *BeppoSAX* is sensitive to photon energies up to 10.5 keV, and has a half-power radius that is one-half that of the *ASCA* GIS instrument. In addition, the PSF of *BeppoSAX* is only weakly dependent on energy. Thus, *BeppoSAX* is better-suited for determining temperature profiles for clusters of galaxies than previous X-ray telescopes. Using a sample of 11 clusters found in the *BeppoSAX* archive, we derive radial temperature profiles for each cluster. In a future paper, we will discuss the abundance profiles of the 11 clusters. Throughout this paper, we assume $H_0 = 50 \text{ km s}^{-1} \text{ Mpc}^{-1}$ and $q_0 = 0.5$.

2. SAMPLE AND DATA REDUCTION

From the *BeppoSAX* Science Data Center (SDC) archive (available at http://www.sdc.asi.it/sax_main.html) we have obtained data for seven cooling flow clusters (A85, A496, A1795, A2029, A2142, A2199, and 2A0335+096) and four non-cooling flow clusters (A2163, A2256, A2319, and A3266). All the clusters have redshifts in the range $z = 0.03 - 0.09$ except A2163 ($z = 0.203$). We analyze data from the Medium Energy Concentrator Spectrometer (MECS), which consists of three identical gas scintillation proportional counters (two detectors after 1997 May 9) sensitive in the 1.3–10.5 keV energy range. A detailed description of the MECS is given in Boella et al. (1997). The event files were subjected to the standard screening criteria of the *BeppoSAX* SDC.

¹Chandra Fellow.

Since our goal is spatially-resolved spectroscopy, accounting for scattering from the PSF of the MECS is important. As stated above, scattering from the PSF has an enormous impact on the temperature profiles derived from *ASCA* data. Fortunately, the detector + telescope PSF of *BeppoSAX* is nearly independent of energy, unlike the *ASCA* GIS. This is because the Gaussian PSF of the MECS detector improves with increasing energy, while the PSF of the grazing incidence Mirror Unit degrades with increasing energy (D’Acri, De Grandi, & Molendi 1998), leading to a partial cancellation when these two effects are combined. Still, it is important to account for the PSF accurately when deriving temperature profiles.

To correct for the PSF we have used the routine *effarea*, available as part of the SAXDAS 2.0 suite of *BeppoSAX* data reduction programs. This routine is described in detail in Molendi (1998) and D’Acri et al. (1998). Briefly, *effarea* creates an appropriate effective area file that corrects for vignetting and scattering effects for an azimuthally-symmetric circular or annular region. It does so by creating correction vectors that are a function of energy, and which when multiplied by the observed spectrum yields the corrected spectrum. The surface brightness profile of the cluster (determined from the analysis of *ROSAT* data by Mohr, Mathiesen, & Evrard 1999 and Ettori & Fabian 1999) is convolved with the PSF of the MECS in order to determine the extent to which scattering from other regions of the cluster have contaminated the emission from the extraction region in question. This information is incorporated into the auxiliary response file (the *.arf* file), which is subsequently used in the spectral fitting. The correction to the observed spectrum is modest; D’Acri et al. (1998) and Kaastra, Bleeker, & Mewe (1998) found only small changes between the uncorrected and corrected temperature profiles for Virgo and A2199, respectively. The mismatch in energy bandpasses between the *ROSAT* (0.2–2.4 keV) surface brightness profile and *BeppoSAX* (1.65–10.5 keV) does not appear to have significantly affected the results.

For each cluster, spectra were extracted from concentric annular regions centered on the peak of emission of the cluster with inner and outer radii of $0' - 2'$, $2' - 4'$, $4' - 6'$, and $6' - 9'$. We also extracted one global spectrum from $0' - 9'$. At $9'$ the telescope entrance window support structure (the strongback) becomes a factor. In addition, for off-axis angles greater than $10'$, the departure of the PSF from radial symmetry becomes noticeable (Boella et al. 1997). This coupled with the fact that some of the clusters have poor photon statistics outside of $10'$ prompted us to end our profiles at $9'$. At this radius, our temperature profiles extend out to 55% of the virial radius, r_{virial} , for A2163 and 17%–33% for the other clusters, where $r_{\text{virial}} = 3.9 (T/10 \text{ keV})^{1/2} \text{ Mpc}$. Background was obtained from the deep blank sky data provided by the SDC. We used the same region filter to extract the background as we did the data, so that both background and data were affected by the detector response in the same manner. The energy channels were rebinned to contain at least 25 counts.

The procedure outlined above does not fit the spectrum of the various regions within the cluster simultaneously. Instead, it assumes a uniform spectrum throughout when

correcting for contamination from other regions. Whereas this is not important for the innermost bin (since very few photons are scattered in from larger radii compared to the number of photons truly belonging in the innermost bin), this might affect the outer bins if the temperature profile is varying strongly. This does not seem to be the case though. The spectrum correction vectors presented in D’Acri et al. (1998) for A2199 were quite modest. Other than their innermost bin (which loses some flux via scattering but does not receive much scattered flux from exterior bins), the corrections amounted to 5% or less for energies above 3 keV. In addition, if the exterior bins were significantly contaminated by emission from the interior of the cluster that was at a considerably different temperature, it is likely that no single-component thermal model would give an adequate fit to the data. However, all the spectral fits of the third and fourth spatial bins of the clusters in our study were adequate, with nearly all fits having $\chi_\nu < 1.05$. This coupled with the fact that the PSF-corrected temperatures were not significantly different from the uncorrected temperatures (see § 3.2) indicates that our results are not strongly affected by not fitting the spectra from different regions simultaneously.

For one of the lower temperature clusters (A2199) a long pointed *ROSAT* PSPC observation was available in the HEASARC archive for which no *ROSAT*-determined temperature profile had been published. The observation (RP800644N00) was filtered such that all time intervals with a Master Veto Rate above $170 \text{ counts s}^{-1}$ were excluded, in order to discard periods of high background. This resulted in a net exposure of 34,232 seconds. Background was taken from an annulus with inner and outer radii of $30'$ and $40'$. The background was scaled to and subtracted from the source spectra, which were subsequently binned such that each energy channel contained at least 25 counts. Energy channels below 0.2 keV were ignored in the fit.

3. TEMPERATURE OF THE HOT GAS

3.1. Global Temperatures

Using XSPEC we used a MEKAL model with an absorption component fixed at the Galactic value in all spectral fits, except the *ROSAT* PSPC observation of A2199. The temperature, metallicity, and redshift were allowed to vary. Spectral fits of *BeppoSAX* MECS data of the Perseus cluster with the redshift fixed showed significant residuals in the iron line complex region around 6.7 keV (R. Dupke 1999, private communication). These residuals disappeared when the redshift was allowed to vary. The cause of this feature is a systematic shift of 45–50 eV in the MECS channel-to-energy conversion (F. Fiore 1999, private communication). This systematic shift was evident in our sample; when the redshift was allowed to vary, the measured redshift was less than the optically-determined redshift in all 11 clusters, and inconsistent with the optically-determined redshift at the 90% confidence level for eight of them. A modest decrease in the reduced χ^2 also occurred for most of the clusters when the redshift was allowed to vary. However, freeing the redshift did not affect the values obtained for the temperature and metallicity significantly (less than a 5% change in either quantity).

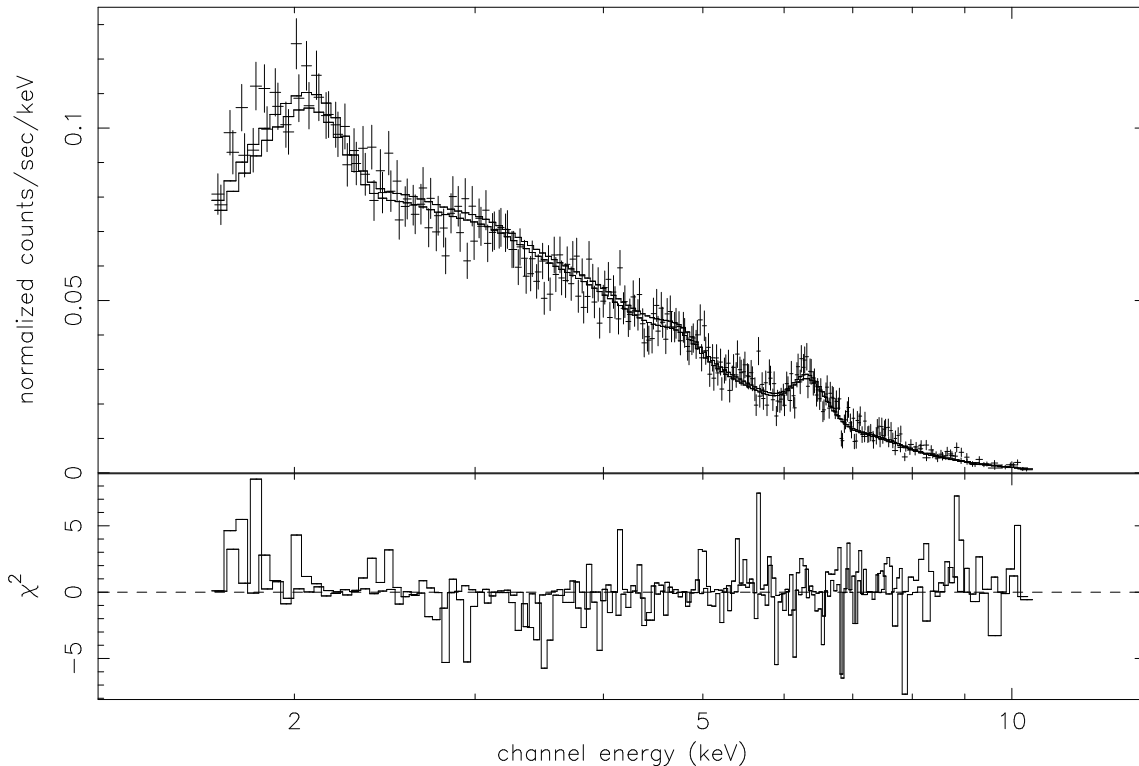


Fig. 1.— Best-fit MEKAL model spectrum with residuals to the global spectrum of the non-cooling flow cluster A2256 using data in the 1.65–10.5 keV range. An excess of positive residuals below 3.0 keV was a feature common in all 11 clusters analyzed here.

With the model described above, we fit the data from MECS2 and MECS3 (and MECS1 when available) separately, but with the same normalization. In accordance with the *Cookbook for BeppoSAX NFI Spectral Analysis* energy channels below 1.65 keV and above 10.5 keV were ignored in the fit. On the whole, the fits to the global spectra were rather poor, ranging from $\chi^2_\nu = 1.13 - 1.8$ for 170–556 degrees of freedom. Inspection of the residuals revealed that the poor fits resulted from excess emission in the 1.65–3.0 keV range. The best-fit spectrum from the non-cooling flow cluster A2256 is shown in Figure 1 and illustrates the positive residuals below 3.0 keV. This effect was even more pronounced in the cooling flow clusters. We performed the fits again, this time only using data in the 3.0–10.5 keV range. The fits were much better, with the fits to all clusters having $\chi^2_\nu \leq 1.20$. In addition, the global temperature values for the fits performed in the 3.0–10.5 keV range were much closer to the global values determined from *ASCA* data (see Table 1). Ten of the 11 temperatures derived from the 1.65–10.5 keV fit were below the *ASCA* value, and in eight cases the 90% error bars did not overlap. Conversely, nine of the 11 temperatures derived from the 3.0–10.5 keV fit have 90% error bars that overlap with the error bars from the *ASCA* temperatures. All quoted errors are 90% confidence levels unless otherwise noted.

Since the improvement in χ^2_ν when channels in the 1.65–3.0 energy range were excluded was more pronounced for the cooling flow clusters than in the non-cooling flow clusters, we investigated the possibility that the excess emis-

sion below 3.0 keV was a result of a cooling flow component. Indeed, the addition of a cooling flow model to the MEKAL model provided a substantially better fit in the 1.65–10.5 keV case, and in some cases the fit became formally acceptable. However, the inferred cooling rates were several hundred solar masses per year higher than previous published values (e.g., Peres et al. 1998). In fact, cooling rates of several hundred solar masses per year were found for the non-cooling flow clusters A2163, A2256, A2319, and A3266. In addition, significant cooling rates were found for spectra extracted from regions of the cluster far from the cluster center, where no cooling gas should be found. This clear contradiction illustrates how a physically implausible model can still yield good spectral fits, and the danger in interpreting such a result. We conclude that although some of the excess emission in the 1.65–3.0 keV range is from cooling gas, there is a clear excess of soft emission beyond what is expected from cooling gas, possibly due to uncertainties in the calibration of the MECS instruments. Since including this energy range leads to global temperatures significantly below the *ASCA* value, we only fit the data in the 3.0–10.5 keV range for the remainder of the paper. Given the good agreement in the 3.0–10.5 keV fit and the *ASCA*-determined temperatures, we are confident of the calibration of *BeppoSAX* above 3.0 keV.

3.2. Radial Temperature Profiles

The PSF-corrected and -uncorrected radial temperature profiles for each of the 11 clusters are shown in the left pan-

Table 1:

GLOBAL TEMPERATURE FITS					
Cluster	<i>ASCA</i> ^a	1.65–10.5 keV		3.0–10.5 keV	
	kT (keV)	kT^b (keV)	χ_ν /d.o.f.	kT^b (keV)	χ_ν /d.o.f.
A85	6.1 ± 0.2	$5.6^{+0.1}_{-0.1}$	1.70/340	$6.4^{+0.3}_{-0.2}$	1.17/282
A496	4.3 ± 0.2	$3.7^{+0.1}_{-0.1}$	1.59/317	$4.2^{+0.1}_{-0.1}$	1.20/259
A1795	6.0 ± 0.3	$5.0^{+0.2}_{-0.2}$	1.14/269	$6.0^{+0.4}_{-0.4}$	0.97/211
A2029	8.7 ± 0.3	$6.7^{+0.2}_{-0.2}$	1.26/170	$7.6^{+0.5}_{-0.4}$	0.98/141
A2142	8.8 ± 0.6	$7.6^{+0.2}_{-0.2}$	1.32/350	$8.7^{+0.4}_{-0.4}$	1.02/292
A2163	11.5	$11.0^{+0.6}_{-0.6}$	1.32/556	$11.7^{+1.0}_{-0.9}$	1.05/440
A2199	4.4 ± 0.2	$4.0^{+0.1}_{-0.1}$	1.58/506	$4.4^{+0.1}_{-0.1}$	1.03/419
A2256	7.5 ± 0.4	$6.2^{+0.3}_{-0.3}$	1.13/296	$7.1^{+0.5}_{-0.4}$	1.06/238
A2319	9.2 ± 0.7	$8.8^{+0.3}_{-0.4}$	1.27/331	$10.5^{+0.8}_{-0.7}$	1.04/273
A3266	7.7 ± 0.8	$8.0^{+0.4}_{-0.3}$	1.15/323	$9.9^{+0.8}_{-0.7}$	0.93/265
2A0335+096	$\sim 3.4^c$	$2.80^{+0.03}_{-0.04}$	1.80/315	$3.20^{+0.08}_{-0.08}$	1.13/257

^aSingle-fit temperature from Markevitch et al. (1998).

^bErrors listed are 90% confidence levels.

^cEstimated value inside of $10'$ from radial temperature profile of Kikuchi et al. (1999).

els of Figure 2. As was found in previous studies, correction for the MECS PSF does not seriously affect the temperature profile. In the right panels are our *BeppoSAX* temperature profiles along with temperature profiles derived from other *ASCA* and *BeppoSAX* studies for comparison. We note that for A85, A496, A1795, A2029, A2142, and A2199 the innermost bin has been fit with a cooling flow component in addition to a thermal model for the profiles of Markevitch et al. (1998), Markevitch et al. (1999), and Sarazin, Wise, & Markevitch (1998), which accounts for the large discrepancy in this bin compared to other studies that fit the spectra with only single-component models.

A85: We have included the subclump to the south of the cluster center in our analysis. Outside of the cooling radius, the temperature profile increases moderately from 6.4 keV to 7.9 keV at a significance level of 2.2σ . This is in agreement with the *ASCA* analysis by White (1999), but contrasts with Markevitch et al. (1998) who found a profile that decreased from 8.0 keV in a $1'5 - 6'$ annular bin to 6.3 keV in a $6' - 12'$ annular bin with *ASCA* data. Pislar et al. (1997) and Kneer et al. (1995) analyzed *ROSAT* PSPC data for this cluster and found a roughly isothermal profile outside the cooling region. However, the *ROSAT* analysis found a significantly lower temperature, with most of the cluster below 5 keV. This is possibly due to a gain calibration problem of the *ROSAT* PSPC instrument.

A496: This nearby cluster ($z = 0.0326$) has a cooling rate of $\dot{M} = 95 M_\odot \text{ yr}^{-1}$ (Peres et al. 1998). The temperature is lowest in the center (typical of a cooling flow), and is consistent with a constant value of 4.5–5.0 keV at larger radii. This is consistent with the *ASCA* analysis of Dupke & White (1999), who did not perform a PSF correction. For low temperature clusters, the PSF does not introduce a significant spurious positive gradient to the temperature profile (Takahashi et al. 1995). The profile of White (1999) also agreed for the most part with our

profile, although one of their bins deviated by $\sim 2\sigma$ from ours. Markevitch et al. (1999) found a continuous drop in temperature of 5.6 keV to 3.5 keV from a $2' - 5'$ annular bin to a $10' - 17'$ annular bin.

A1795: We find a temperature profile consistent with a temperature of 6–7 keV outside of the cooling flow region. A significant decrease in temperature was not found in the center for this cooling flow cluster. This result is similar to the *ASCA* results of Mushotzky et al. (1995; uncorrected for the PSF), White (1999), and Ohashi et al. (1997), although the Ohashi et al. (1997) result found a somewhat lower overall temperature for this cluster. Markevitch et al. (1998) detected a decline in temperature with radius, but not at a high significance with *ASCA*. *ROSAT* found a low temperature in the inner cooling flow region, and a moderately increasing profile at larger radii (Briel & Henry 1996). The discrepancy in the innermost bin is likely the result of the low energy bandpass (0.1–2.4 keV) of *ROSAT* sampling lower temperature gas than the higher energy bandpass (3.0–10.5 keV) of *BeppoSAX* in the cooling region.

A2029: We find a basically flat temperature profile out to $6'$ and a marginally significant (1.7σ) rise from $6' - 9'$, consistent with the *ASCA* analysis of White (1999). This is the opposite trend found by Sarazin et al. (1998) with *ASCA* data, who found a decline in temperature from ~ 9 keV to 6 keV outside of $5'$ (but with large errors in the outer regions). Still, they found that an isothermal profile was rejected at the $> 96\%$ confidence level. This was one of the few clusters for which Irwin et al. (1999) found evidence for a statistically significant temperature decline with *ROSAT* data, although the drop did not occur until outside of $10'$. Molendi & De Grandi (1999) analyzed the same *BeppoSAX* data and found a temperature profile consistent with 8 keV out to $8'$ and dropping to 5 keV from $8' - 12'$ (see § 4.3 for a detailed comparison of the two analyses).

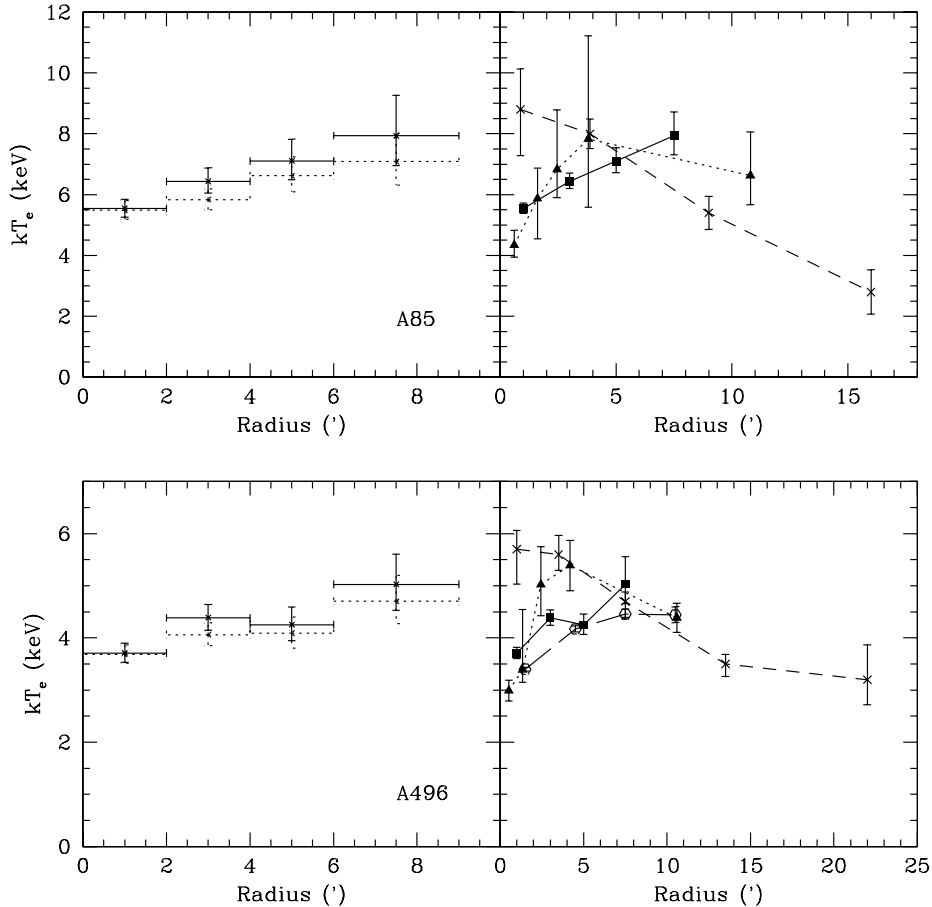


Fig. 2.— Radial temperature profiles for the 11 clusters in the sample, derived from fitting in the 3.0–10.5 keV range. In the left panel, solid lines represent temperatures corrected for the PSF of *BeppoSAX* and the dotted lines are not corrected. Error bars are 90% confidence levels. The right panels compare our results (filled squares and solid lines) with temperature profiles derived from *ASCA* data using the method of White (1999; filled triangles and dotted line), the method of Markevitch et al. (1996; crosses and dashed lines), uncorrected *ASCA* profiles from Dupke & White (1999) and Kikuchi et al. (1999) (open hexagons and long dashed line in A496 and 2A0335+096), and *BeppoSAX* profiles for A2029, A2199, A2319, and A3266 (open triangles and long dashed lines). For the right panels, the error bars are 1σ confidence levels.

A2142: We find a very flat profile with a temperature of 8–9 keV. A similar result was found by White (1999), although the errors were large. Markevitch et al. (1998) found evidence for a temperature decline, but not at a high significance level. Henry & Briel (1996) analyzed *ROSAT* data and found temperatures of 10 keV or higher outside the cooling region, with a peak in the 2.5–5' bin.

A2163: This cluster has the highest redshift in our sample ($z = 0.203$), and is also the hottest. The cluster does not possess a cooling flow and probably underwent a merger in the recent past (e.g., Elbaz, Arnaud, & Böhringer 1995). Since the centroid of the cluster lies over 5' from the detector center, we have excluded data from behind the strongback support structure and beyond. We have included data in the last annular bin out to 12' (as long as it fell inside the strongback) to improve the statistics in the last bin. Our profile extends out to 73% of the virial radius, considerably farther than any other cluster in our sample. We find that the cluster has a temperature of 10–11 keV out to 4', before experiencing a marginally significant ($< 2\sigma$) rise in temperature at larger radii. The errors are quite large at large radii, although the tem-

perature is greater than 8 keV at the 90% level. This agrees with the *ASCA* result of White (1999), but disagrees strongly with the result from *ASCA* and *ROSAT* by Markevitch et al. (1996), who found temperatures of $12.2^{+1.9}_{-1.2}$, $11.5^{+2.7}_{-2.9}$, and $3.8^{+1.1}_{-0.9}$ for annular bins of 0'–3', 3'–6', and 6'–10' in extent, respectively. For these regions, we find temperatures of $10.1^{+0.9}_{-0.8}$, $11.7^{+2.6}_{-1.8}$, and $13.2^{+17.9}_{-4.6}$, respectively, using only data inside the strongback (90% errors). Thus, the outermost bin of the *BeppoSAX* data differs from that of Markevitch et al. (1998) at the 3.3σ confidence level.

A2199: Outside of the cooling flow region, we find a constant temperature of about 4.5 keV. Analysis of the same *BeppoSAX* data by Kaastra et al. (1998) and of *ASCA* data by White (1999) found a similar result. However, Markevitch et al. (1999) found a steadily decreasing profile from 5.2 keV to under 5 keV at 7.5', with a further decline at larger radii with the same *ASCA* data.

We have analyzed the *ROSAT* PSPC data for this cluster, and derived a temperature profile out to 18' (0.9 Mpc). The angular extent of this cluster is large, so to confirm that our background region was not significantly contam-

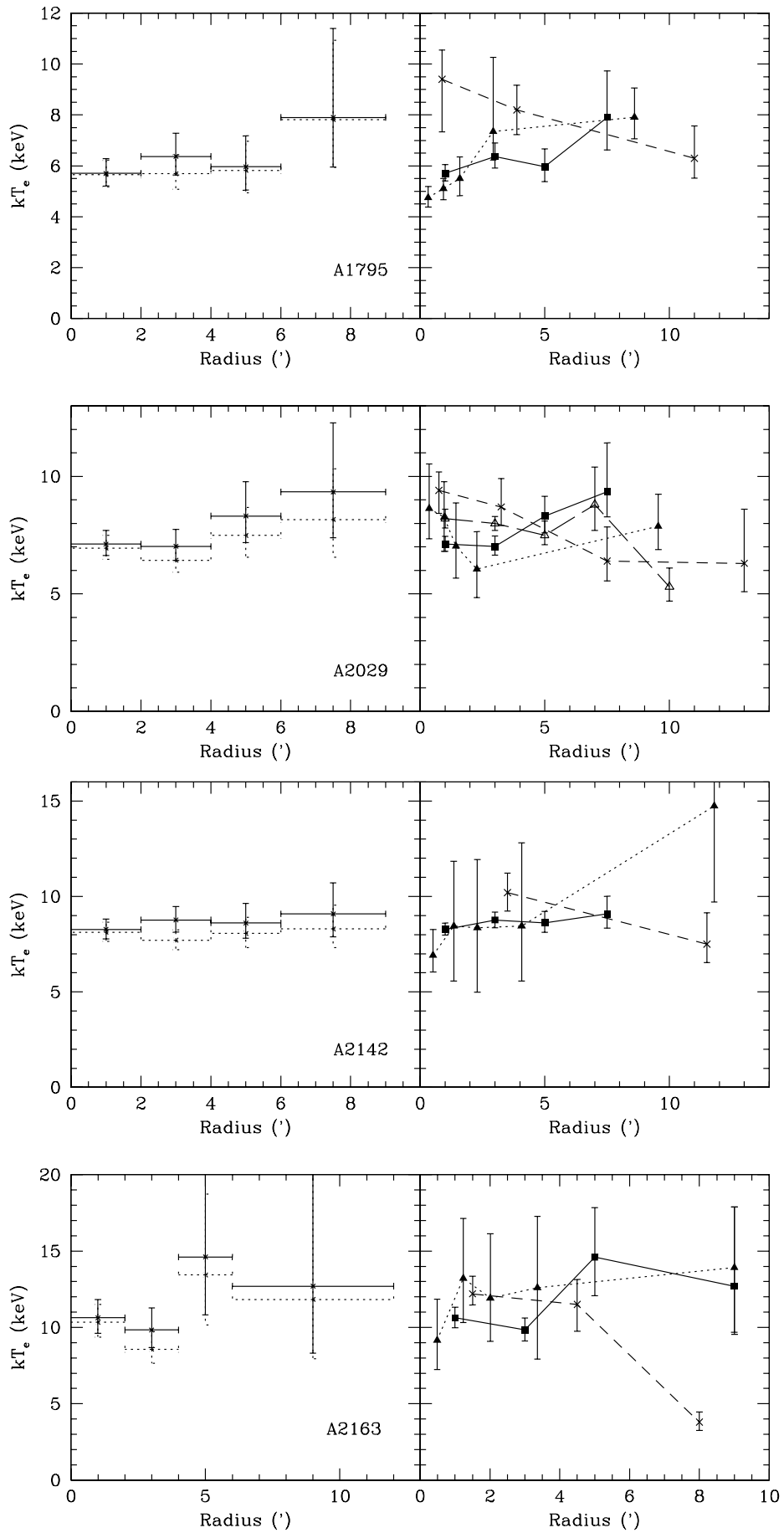


Fig. 2 – continued.

inated by the cluster emission, we derived a temperature

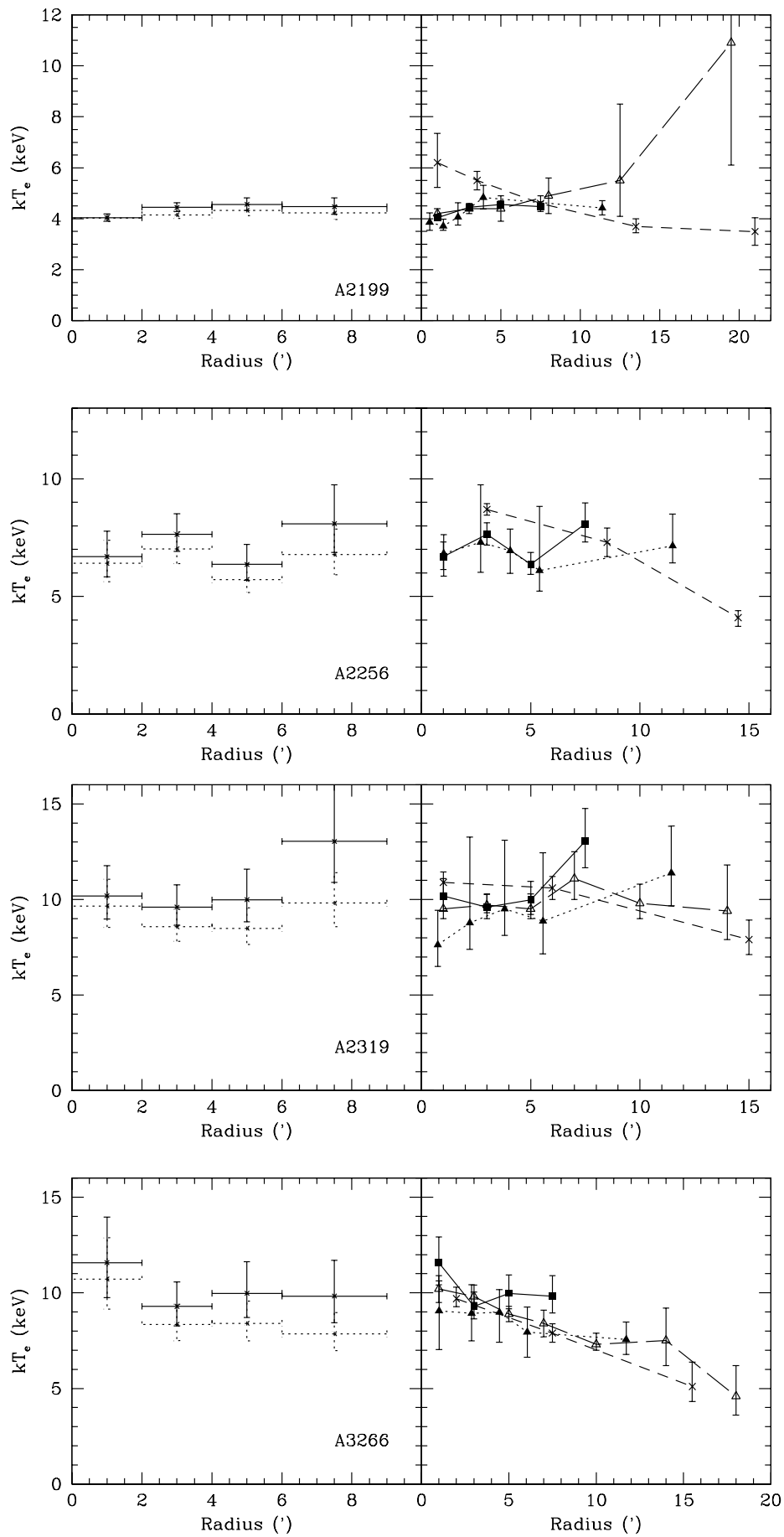


Fig. 2 – continued.

profile using a background annulus of $40' - 50'$ and found

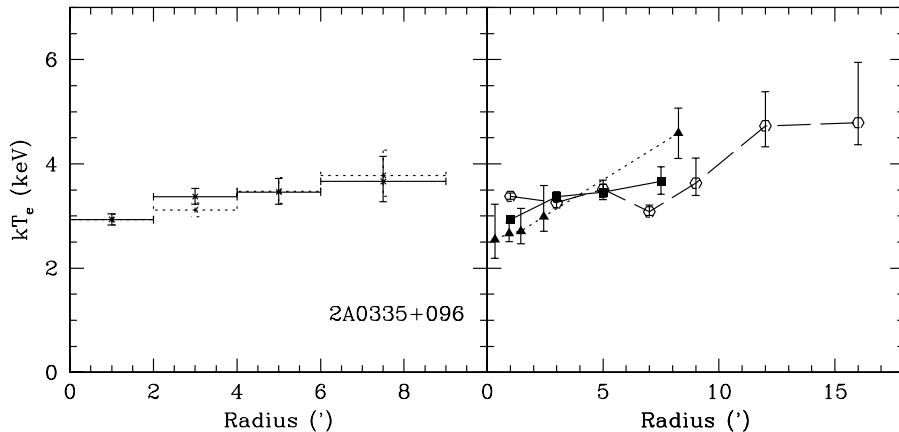


Fig. 2 – continued.

the same results as we did with a background annulus of $30' - 40'$. The temperature profile is shown in Figure 3. The profile shows a drop in the center indicative of a cooling flow. At large radii the profile is flat. However, the *ROSAT*-derived temperature is significantly lower than the value from *ASCA* or *BeppoSAX*. Whereas this might be expected in the central cooling flow region where *ROSAT* is sampling cooler gas than the other instruments because of its low energy bandpass, this tendency persists outside the cooling region. From $2' - 9'$, the temperature is 3.2 ± 0.2 keV, whereas it is 4.5 ± 0.1 for *BeppoSAX*. Data from *ROSAT* appears sometimes to have a tendency to measure lower temperatures than other instruments for clusters, such as A3558 (Markevitch & Viklinin 1997) and A85 (see above).

To compensate for this effect, we have adjusted the gain of the observation such that the temperature in the $2' - 9'$ region matched that of *BeppoSAX*. We excluded the inner $2'$ to avoid complications from the cooling flow region. An adjustment of 1.5% in the gain was necessary to bring the global temperature determined by the two instruments into agreement. A gain adjustment of this magnitude was within the range of values found by Henry & Briel (1996) when they analyzed five different pointings of A2142 with *ROSAT*. With this new gain value the temperature profile remains flat outside of the cooling region out to $18'$ (35% of the virial radius), albeit at a higher value than before. The main conclusion drawn from the *ROSAT* result of A2199 is that the temperature profile appears flat outside of the cooling flow region regardless of whether or not the gain was adjusted.

A2256: We find a flat temperature profile consistent with a temperature of 7 keV, in excellent agreement with the *ASCA*-determined profile of White (1999). This contrasts with the Markevitch (1996) result from *ASCA* which found the temperature to decrease from 8.7 keV to 7.3 keV from the $0' - 6'$ to $6' - 11'$, with a steep drop to 4 keV at larger radii. Markevitch (1996) claims that the *ROSAT* data confirm this result, albeit with larger errors, contrary to the claim of Briel, & Henry (1993) who analyzed the same *ROSAT* data and found a roughly isothermal profile.

A2319: We find a flat temperature profile out to $6'$ and a marginally significant ($\sim 2\sigma$) increase from $6' - 9'$.

This is consistent with the White (1999) result. Markevitch (1996) also found an isothermal profile out to $10'$ with *ASCA*, and a decreasing profile at larger radii. The *ROSAT* data suggested isothermality (Irwin et al. 1999). Molendi et al. 1999 analyzed the same *BeppoSAX* data and found a flat temperature profile out to $16'$.

A3266: This probable merging cluster exhibits a slight increase in temperature in the center and levels off at radii out to $9'$. With *ASCA* data, Markevitch et al. (1998) found a steady decrease in temperature from almost 10 keV in the central 2.5 to 5 keV outside of $10'$, and White (1999) also found a modestly decreasing profile (from 9 keV to 7.5 keV). The *ROSAT* data suggested isothermality although a modest decrease in temperature could not be ruled out (Irwin et al. 1999). De Grandi & Molendi (1999) analyzed the same *BeppoSAX* data and found a more substantial decrease in temperature, with a drop from 10 keV in the center to 4.5 keV out to $20'$.

2A0335+096: The coolest cluster in our sample, 2A0335+096 possesses a rather strong cooling flow ($400 M_{\odot} \text{ yr}^{-1}$; Irwin & Sarazin 1995). The temperature is lowest in the innermost bin and levels off to a value of 3.4 keV out to $9'$. Kikuchi et al. (1999) analyzed the *ASCA* data for this cluster and found a flat temperature profile out to $10'$, while White (1999) found a flat profile out to $4'$ and a jump to 4.6 keV at larger radii.

In conclusion, the temperature profiles of the 11 clusters in our sample are roughly constant, and in general agreement with those derived from *ASCA* data by White (1999). This is in disagreement with the profiles derived from the same *ASCA* data with the method of Markevitch et al. (1996), which find a significant decrease in temperature in many of the clusters. A more detailed comparison is given in § 4.

3.3. Normalized Temperature Profiles

In Figure 4a we plot the temperature profiles normalized to the global temperature for all 11 clusters versus radius in units of the virial radius, r_{virial} . The error bars represent the 1σ uncertainties. At small radii, the normalized profiles are typically less than one, owing to the presence of cooling flows in seven of the 11 clusters. As a result of the low temperature in the center, the outer regions are

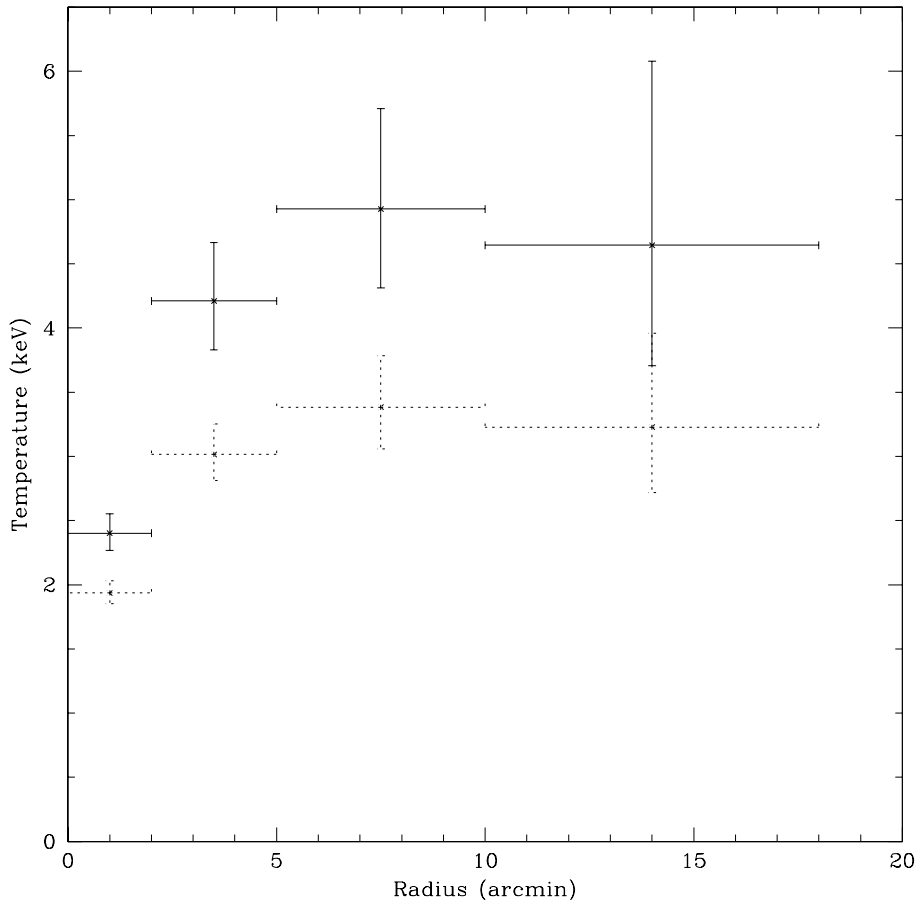


Fig. 3.— Temperature profile of A2199 derived from the *ROSAT* PSPC with 90% error bars. Outside of the cooling radius, the temperature profile is flat both in the case where the gain is set to the nominal value (dotted line) or adjusted such that the temperature in the 2' – 9' region is normalized to the temperature derived from *BeppoSAX* for the same region (solid line).

necessarily normalized to a value greater than one. To compensate for this effect, we have calculated global temperatures for the seven cooling flow clusters excluding the inner 2', and then normalized the 2' – 4', 4' – 6', and 6' – 9' bins by this temperature, while excluding the innermost bin. The result is shown in Figure 4*b*. Out to 20% of the virial radius, the temperature profiles appear flat. From 20% to 30% of the virial radius, the profiles rise somewhat, although the temperatures are not well constrained in this region. Most of the values are consistent with unity at the 1σ confidence level.

A constant temperature model ($T/T_{mean} = 1$) provided a good fit to the data ($\chi^2 = 43.7$ for 37 degrees of freedom). A linear model of the form $(T/T_{mean}) = a + b(r/r_{virial})$ provided a somewhat better fit ($\chi^2 = 36.0$ for 35 degrees of freedom), with values of $a = 0.942$ and $b = 0.440$. The 90% confidence range on the slope b was 0.123–0.752. This best-fit line is shown in Figure 4*b*, with the dashed lines representing the 90% confidence levels on the slope of the line. We find that a temperature drop of 14% from the center out to 30% of the virial radius can be ruled out at the 99% confidence level.

The data indicate that the gas is isothermal or mildly increasing in temperature out to 30% of the virial radius ($1.0h_{50}^{-1}$ Mpc for a 7 keV cluster). Beyond this radius, the temperature profile may well decline. Most hydrodynamical

cluster simulations predict a drop in temperature past 50% of the virial radius (see, e.g., Frenk et al. 1999). *XMM* will be the ideal instrument for determining the temperature profiles of clusters at large radii.

4. COMPARISON TO OTHER RESULTS

The presence of temperature gradients in clusters of galaxies has been a topic of hot debate in recent years, and there have been many investigations as to the temperature structure of clusters. Here, we summarize previous results grouped by X-ray telescope and compare them to our results.

4.1. Temperature Profiles Determined With *ASCA*

The claim of the existence of large temperature declines with radius was first suggested following the results from *ASCA* data using the PSF-correction technique of Markevitch et al. (1996), including Markevitch (1996), Markevitch et al. (1998), Sarazin et al. (1998), and Markevitch et al. (1999). Markevitch et al. (1998) observed 30 clusters with *ASCA* and found in general that the temperature profiles declined with radius (up to a factor of two), and that the decline was described well by a polytropic equation of

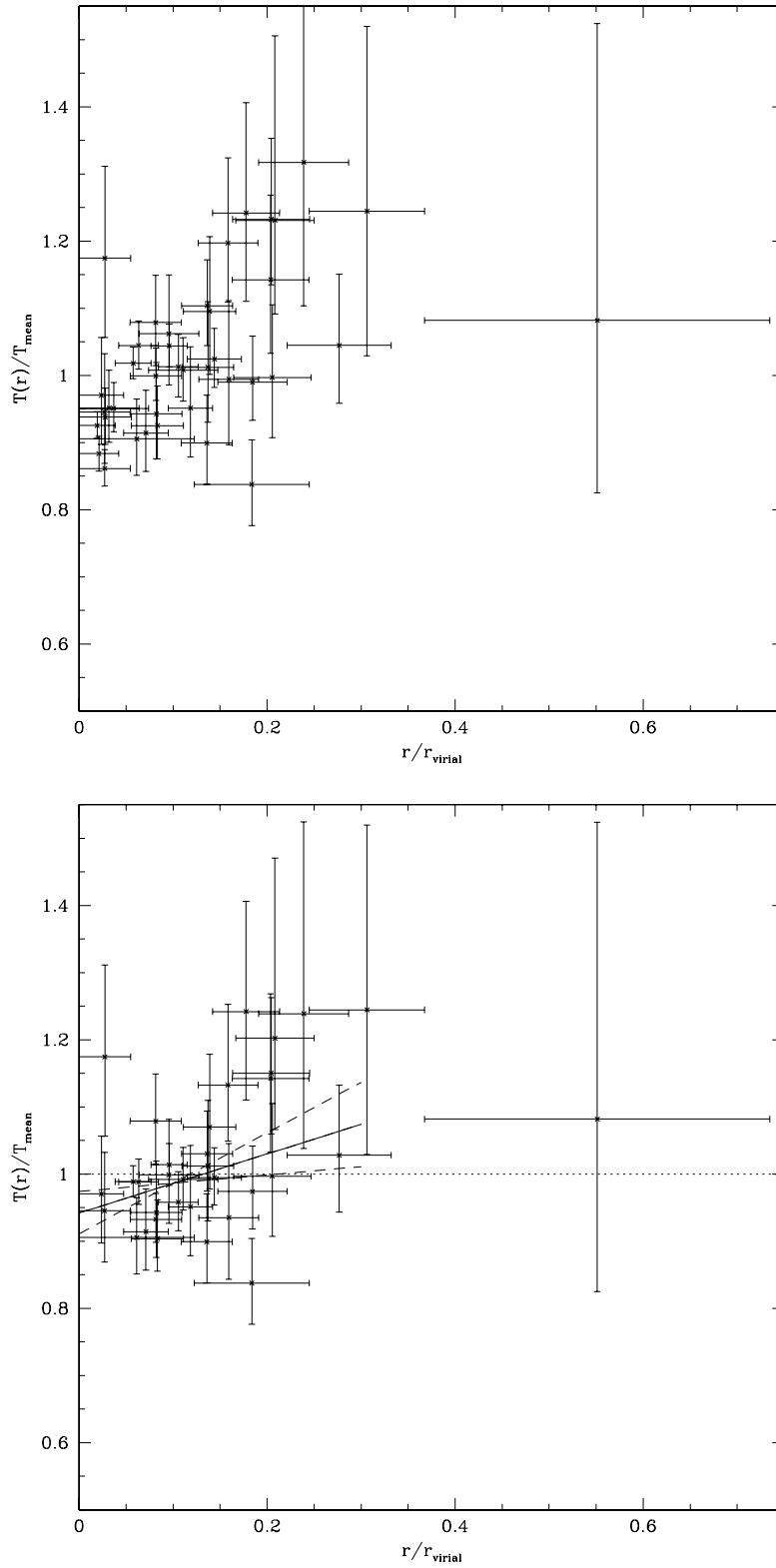


Fig. 4.— (a) Normalized temperature profiles for all 11 clusters in the sample versus radius in units of the virial radius. (b) Normalized temperature profiles after compensating for the effects of cooling flows (see text). Error bars represent the 1σ errors. The solid line is the best-fit linear function, with the dotted lines representing the 90% confidence levels of the slope.

state, i.e.,

$$T(r) \propto \left(1 + \frac{r^2}{a_x^2}\right)^{-3\beta(\gamma-1)/2}, \quad (1)$$

where r is the projected distance, a_x is the core radius, β has its usual meaning in the context of isothermal β -models, and γ is the polytropic index. The best-fit polytropic index was $\gamma = 1.24^{+0.20}_{-0.12}$ (90% confidence levels). This model clearly does not fit the *BeppoSAX* data. The polytropic fit led to $\chi^2 = 577$ for 37 degrees of freedom.

It was pointed out by Irwin et al. (1999) that the trend in the temperature profile found by the method of Markevitch et al. (1996) differed from that found by other PSF-correction techniques from various authors (e.g., Ikebe 1995; Fujita et al. 1996; Kikuchi et al. 1999). Of the 28 clusters analyzed using the method of Markevitch et al. (1996) that did not show very strong evidence for a merger, 22 (14) of them were inconsistent with a constant temperature profile at the 70% (90%) probability level. Conversely, clusters analyzed using the method of Ikebe (1995), Fujita et al. (1996), or Kikuchi et al. (1999) were found to have basically flat temperature profiles, with all 11 clusters consistent with a constant temperature.

Of particular interest are clusters analyzed by more than one method, or clusters whose temperature is low enough that the PSF of *ASCA* does not influence the temperature profile significantly (for clusters below 5 keV). A399, A401, MKW3S, A1795, and A496 are examples where the method of Markevitch et al. (1996) leads to different trends in the radial temperature profiles than with other methods (Fujita et al. 1996; Kikuchi et al. 1996; Ohashi et al. 1997; Dupke & White 1999). The latter two are also in our sample, and show no evidence for a decline in temperature outside of the cooling region (Figure 2).

Recently, White (1999) has determined the temperature profiles of a large number of clusters observed with *ASCA* using the PSF-correction technique outlined in White & Buote (1999). He found that 90% of the 98 clusters in his sample were consistent with isothermality at the 3 σ confidence level. On a cluster by cluster comparison of the 11 clusters common in both samples, we find our temperature profiles are in excellent agreement with those of White (1999), with only two exceptions. Our temperature value of the outermost bin of A3266 is ~ 2 keV higher than the value of White (1999). However, the 1σ error bars just touch so this discrepancy is not at a high significance. Also, our temperature profile of A496 differs somewhat from his. This difference occurs around $4'$ and is significant at $\sim 2\sigma$. However, given that we have 44 temperature values for the 11 clusters, it is not unreasonable that two of our values differ by 2σ . In fact, this is the number of 2σ discrepancies one would expect from a statistical point of view.

Given the conflicting results regarding this topic, it is worthwhile to examine the PSF-correction techniques of the two largest studies, namely those using the techniques of Markevitch et al. (1996; hereafter method M) and White & Buote (1999; hereafter method WB). Both techniques assume a spatial distribution for the cluster emission; method M assumes the emissivity profile obtained from *ROSAT* PSPC data for the cluster in question, while method WB assumes the spatial distribution derived from a maximum-likelihood deconvolution of the *ASCA* image. Method M creates simulated events drawn from this spatial distribution and from an initial guess for the cluster spectrum, and convolves the events with

the spatially-variable PSF. The input cluster spectrum is varied until the simulated data matches the actual data. Method WB ray-traces events drawn from the spatial distribution through the telescope optics and attempts to find the most likely association between events in the deconvolved and convolved planes on a PI energy bin by PI energy bin basis. Once an energy has been assigned to each event in the deconvolved plane, the event list can be analyzed via standard spectral-fitting procedures.

Both methods have their advantages and disadvantages. Whereas method WB employs only a spatially-invariant PSF, method M uses a PSF that varies with position. On the other hand, method M is reliant on *ROSAT* data to determine the emissivity profile, while method WB is not. It is not clear if the emissivity profile derived from the 0.2–2.0 keV *ROSAT* band is appropriate for use over the *ASCA* bandpass. The only way to determine which of these disadvantages are leading to incorrect results is to create simulated data with a known temperature and surface brightness profile and convolve it with the response of the instrument, and then see if the PSF-correction technique can recover the input temperature and surface brightness profiles. White & Buote (1999) have tested their code on simulated cluster data with a giant cooling flow model, a medium cooling flow model, an isothermal profile, and a profile that decreases by a factor of two from the center out to $20'$, as well as data of varying signal-to-noise ratios. In all cases, the original temperature and surface brightness profiles are recovered. Conversely, method M has not been as extensively tested on a variety of simulated temperature distributions and signal-to-noise ratios.

As a final note, it should be noted that Markevitch et al. (1998) used a cooling flow model to fit the innermost bin of cooling flow clusters, whereas White (1999) used a single component thermal model. This will naturally lead to a lower value for White (1999) for the innermost bin (typically $\sim 5\%$ of the virial radius). However, White (1999) claims that correcting for the cooling gas leads to an ambient core temperature within the innermost bin consistent with the outer regions of the cluster. Again, this is inconsistent with the results of Markevitch et al. (1998) who find a value for the ambient core temperature greater than the rest of the cluster.

4.2. Temperature Profiles Determined With *ROSAT*

Although the limited bandpass of the *ROSAT* PSPC (0.2-2.4 keV) precludes tight constraints to be put on the temperatures of hot clusters, large (factor of two) temperature changes should be detectable with large enough signal-to-noise ratios. Unfortunately, most clusters observed with *ROSAT* did not have good enough statistics to accomplish this on an individual basis. To circumvent this problem, Irwin et al. (1999) averaged together the radial color profiles (ratio of counts in various bands covering the *ROSAT* PSPC bandpass) of 26 clusters observed with the PSPC. If large-scale deviations from isothermality were common in clusters, such a feature lost in the noise for an individual cluster would become apparent when the clusters were added together. Although a drop in temperature was found in the center of cooling flow clusters (indicating that the method could indeed detect changes in temperatures even for hot clusters), the temperature profiles were

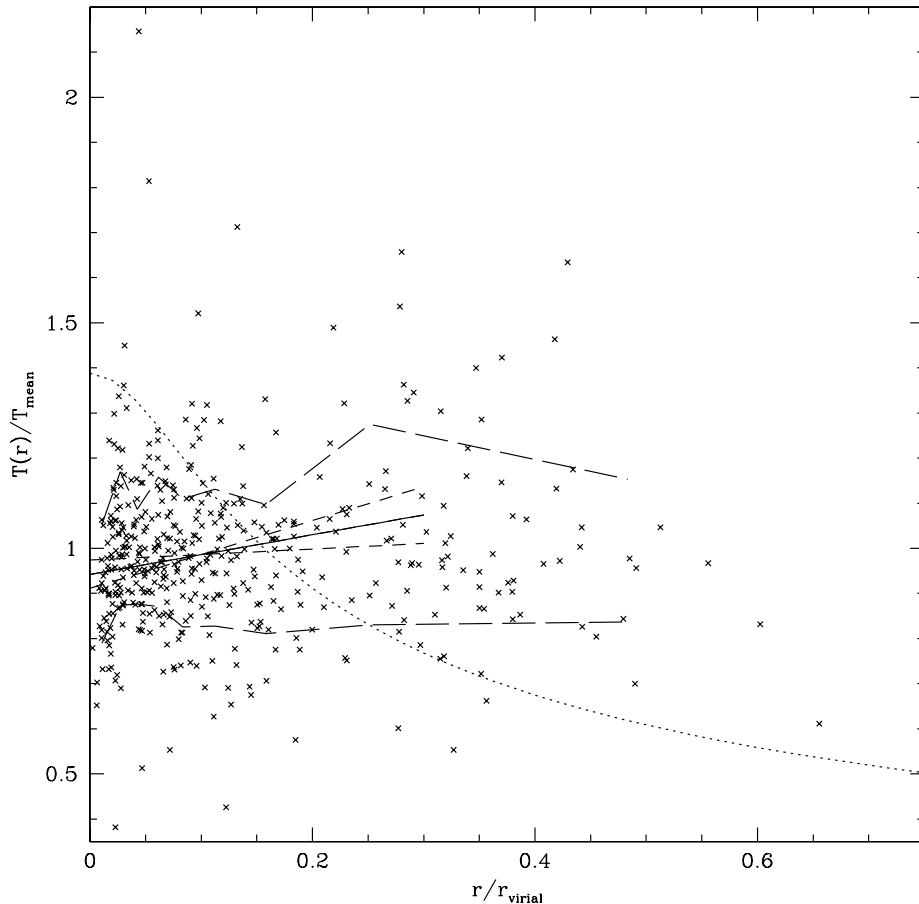


Fig. 5.— Summary of cluster temperature profiles to date. The normalized temperature profiles of 98 clusters observed by White (1999) as a function of the virial radius are shown as crosses. The long dotted lines enclose the middle 68% of the data points. Also shown is the Markevitch et al. (1998) result (dotted line). The solid line with the accompanying dashed lines represents the composite temperature profile presented in this paper along with the 90% errors in the slope of the best-fit line.

flat outside of the cooling region out to 35% of the virial radius. It was found that a 20% temperature drop within 35% of the virial radius was ruled out at the 99% confidence level. This is in agreement with the *BeppoSAX* data presented here, where a decline in temperature of 14% out to 30% of the virial radius is ruled out at the 99% confidence level.

4.3. Temperature Profiles Determined With *BeppoSAX*

Several of the clusters in our sample have been analyzed by other authors: A2199 (Kaastra et al. 1998), A2029 (Molendi & De Grandi 1999), A2319 (Molendi et al. 1999), and A3266 (De Grandi & Molendi 1999). The profile of A2199 is fully consistent with ours. For the other three clusters, somewhat different steps were taken in the data reduction process than what we did. Whereas we excluded data below 3.0 keV, other authors have included data down to 2.0 keV. In addition, they have frozen the redshift whereas we have let it be a free parameter. We have re-analyzed the *BeppoSAX* data for these three clusters, this time including data down to 2.0 keV and freezing the redshift. Although inclusion of channels below 3.0 keV lowered the derived temperatures somewhat (see § 3.1), it did not change the overall shape of the profiles.

Our new profile of A2319 was consistent with that of

Molendi et al. (1999). The profiles of A2029 and A3266 differed somewhat from Molendi & De Grandi (1999) and De Grandi & Molendi (1999). However, the differences occurred only in the 2' – 4' bins, with our 1σ error bars overlapping their 1σ error bars for the other three spatial bins. For both A2029 and A3266 our 2' – 4' temperature was ~ 1.5 keV lower than those obtained by Molendi & De Grandi (1999) and De Grandi & Molendi (1999), and the difference was significant at the 3.3σ and 1.9σ confidence levels for A2029 and A3266, respectively. The cause of this discrepancy may be the choice of the assumed surface brightness profile, especially for the case of A2029, which possesses a large cooling flow. As mentioned in § 2, we have used the double-beta model profile obtained by Mohr et al. (1999) from *ROSAT* PSPC data. It is not stated where the other authors obtained their assumed surface brightness profiles. However, the agreement between the other three spatial bins (especially the first and fourth spatial bins) is encouraging, indicating a flat temperature profile out to 9' for A2029 and A2319, and a modestly decreasing profile for A3266. It should be noted that Molendi & De Grandi (1999) and De Grandi & Molendi (1999) find significant temperature drops in A2029 and A3266, respectively, at very large radii, where we have truncated our profiles because of the presence of the strongback, and

the increasing asymmetry of the PSF at larger radii.

5. A SUMMARY OF CLUSTER TEMPERATURE PROFILES

Given the effort put forth in determining temperature profiles for a large sample of clusters in recent years it is worthwhile to summarize the major contributions to this subject: Markevitch et al. (1998; and references within) and White (1999) with *ASCA* data, Irwin et al. (1999) with *ROSAT*PSPC data, and this current study with *BeppoSAX* data. The combined results are shown in Figure 5. The 98 temperature profiles of White (1999) (shown as crosses) have been normalized to the global temperature for each individual cluster and scaled in units of the virial radius. The long dashed lines enclose the middle 68% of the data points. The error bars are typically rather large for each data point, and have been excluded for clarity. The temperature profile derived by Markevitch et al. (1998) is shown as a dotted line, and represents a fit with polytropic index of $\gamma = 1.24$. The results presented in this paper is shown as a solid line. The *ROSAT*PSPC result is not shown but is very similar to best-fit line derived here, only somewhat less constrained.

The results of White (1999), Irwin et al. (1999), and this study all point to the same general conclusion: outside of the cooling region but inside 30% of the virial radius

there appears to be no decline in the temperature profile. White (1999) extends this result out to 45% of the virial radius, although it should be noted that large drops in the temperature have been found in A2029 and A3266 with *BeppoSAX* data (Molendi & De Grandi 1999; De Grandi & Molendi 1999) in this region. Outside of 45% of the virial radius White (1999) finds evidence for a decline in temperature although the statistics are sparse in this region. This drop is not surprising though since nearly all cluster simulations show a decline in temperature at large radii.

JAI thanks R. Dupke for many useful comments and conversations. We thank D. White for kindly providing us with his *ASCA* temperature profiles, and also the anonymous referee for many insightful comments and suggestions to improve the paper. This research has made use of data obtained through the High Energy Astrophysics Science Archive Research Center Online Service, provided by the NASA/Goddard Space Flight Center, and also the *BeppoSAX* Science Data Center. This work has been supported by *Chandra* Fellowship grant PF9-10009, awarded through the *Chandra* Science Center. The *Chandra* Science Center is operated by the Smithsonian Astrophysical Observatory for NASA under contract NAS8-39073.

REFERENCES

- Boella, G., Chiappetti, L., Conti, G., Cusumano, G., Del Sordo, S., La Rosa, G., Maccarone, M. C., Mineo, T., Molendi, S., Re, S., Sacco, B., & Tripiciano, M. 1997, *A&A*, 122, 327
- Briel, U. G., & Henry, J. P. 1996, *ApJ*, 472, 131
- Briel, U. G., & Henry, J. P. 1994, *Nature*, 372, 439
- D'Acri, F., De Grandi, S., & Molendi, S. 1998, in *The Active X-ray Sky: Results from BeppoSAX and RXTE*, ed. L. Scarsi, H. Bradt, P. Giommi, and F. Fiore (Amsterdam: Elsevier), 581
- De Grandi, S., & Molendi, S. 1999, *astro-ph/9910413*
- Dupke, R. A., & White, R. E., III. 1999, *astro-ph/9902112*
- Ettori, S., & Fabian A. C. 1999, *MNRAS*, 305, 834
- Frenk, C. S., et al. 1999, *ApJ*, 525, 554
- Fujita, Y., Koyama, K., Tsuru, T., & Matsumoto, H. 1996, *PASJ*, 48, 191
- Henry, J. P., & Briel, U. G. 1996, *ApJ*, 472, 137
- Ikebe, Y. 1995, Ph.D. thesis, Tokyo Univ.
- Irwin, J. A., Bregman, J. N., & Evrard, A. E. 1999, *ApJ*, 519, 518
- Irwin, J. A., & Sarazin, C. L. 1995, *ApJ*, 455, 497
- Kaastra, J. S., Bleeker, J. A. M., & Mewe, R. 1998, in *The Active X-ray Sky: Results from BeppoSAX and RXTE*, ed. L. Scarsi, H. Bradt, P. Giommi, and F. Fiore (Amsterdam: Elsevier), 567
- Kikuchi, K., Furusho, T., Ezawa, H., Yamasaki, N., Ohashi, T., Fukazawa, Y., & Ikebe, Y. 1999, *astro-ph/9903431*
- Kneer, R., Böhringer, H., Neumann, D., & Krautter, J. 1996, in *Röntgenstrahlung From the Universe*, ed. H. U. Zimmermann, J. Trümper, & H. Yorke (Garching: MPE), 593
- Markevitch, M. 1996, *ApJ*, 465, L1
- Markevitch, M., Mushotzky, R., Inoue, H., Yamashita K., Furuzawa, A., & Tawara, Y. 1996, *ApJ*, 456, 437
- Markevitch, M., Forman, W. R., Sarazin, C. L., & Vikhlinin, A. 1998, *ApJ*, 503, 77
- Markevitch, M., & Vikhlinin, A. 1997, *ApJ*, 474, 84
- Markevitch, M., Vikhlinin, A., Forman, W. R., & Sarazin, C. L. 1999, *astro-ph/9904382*
- Mohr, J. J., Mathiesen, B., & Evrard, A. E. 1999, *ApJ*, 517, 627
- Molendi, S. 1998, *BeppoSAX* Technical Report, ftp://www.sdc.asi.it/pub/sax/extended_sources.ps.gz
- Molendi, S., & De Grandi, S. 1999, *astro-ph/9910284*
- Molendi, S., De Grandi, S., Fusco-Femiano, R., Colafrancesco, S., Fiore, F., Nesci, R., & Tamburelli, F. 1999, *astro-ph/9909228*
- Mushotzky, R., Loewenstein, M., Arnaud, K., & Fukazawa, T. 1995, in *AIP Conf. Proc. 336, Dark Matter*, ed. S. S. Holdt and C. L. Bennett (New York: AIP), 231
- Ohashi, T., Honda, H., Ezawa, H., & Kikuchi, K. 1997, in *X-ray Imaging and Spectroscopy of Cosmic Hot Plasmas*, ed. F. Makino & K. Mitsuda (Tokyo: Universal Academy), 49
- Peres, C. B., Fabian, A. C., Edge, A. C., Allen, S. W., Johnstone, R. M., & White, D. A. 1998, *MNRAS*, 298, 416
- Pislar, V., Durret, F., Gerbal, D., Lima Neto, G. B., & Slezak, E. 1997, *A&A*, 322, 53
- Sarazin, C. L., Wise, M. W., & Markevitch, M. L. 1998, *ApJ*, 498, 606
- Takahashi, T., Markevitch, M., Fukazawa, Y., Ikebe, Y., Ishisaki, Y., Kikuchi, K., Makishima, K., & Tawara, Y. 1995, *ASCA Newsletter*, #3 (NASA/GSFC)
- White, D. A. 1999, *astro-ph/9909467*
- White, D. A. & Buote, D. A. 1999, *astro-ph/9909457*